Synthetic Poly[(*R*,*S*)-β-hydroxyalkanoates] with Butyl and Hexyl Side Chains

J. J. Jesudason and R. H. Marchessault*

Department of Chemistry, Pulp and Paper Building, McGill University, 3420 University Street, Montreal, Quebec, Canada H3A 2A7

Received May 10, 1993; Revised Manuscript Received November 19, 1993®

ABSTRACT: Synthetic poly[(*R*,*S*)-β-hydroxyheptanoate] (PHH) and poly[(*R*,*S*)-β-hydroxynonanoate] (PHN) were prepared from the ring-opening polymerization of (±)-β-heptanolactone and (±)-β-nonanolactone, respectively, using an *in situ* trimethylaluminum/water catalyst. Molecular weights of about 550 000 and 750 000 for PHH and PHN, respectively, were determined by GPC. Both PHH and PHN are predominantely isotactic "as synthesized"; i.e., the isotacticity diad indices are between 80 and 82%. Amorphous and crystalline regions could be distinguished in the solid-state ^{13}C NMR spectra for both polymers which indicated lower motional freedom for the backbone carbons compared to those in the side chain. Melting points of approximately 60 °C and glass transition temperatures between −30 and −45 °C are close to those of bacterial analogues. The unit cell dimensions of PHH are a = 5.26 Å, b = 31.25 Å, and c = 4.55 Å, based on an orthorhombic unit cell and a $P2_12_12_1$ space group. Compared to poly(β-hydroxybutyrate), the compressed fiber repeat with maintainance of the 2_1 helix is attributed to the intramolecular interactions of the extended alkane side chains.

Introduction

The family of poly(β-hydroxyalkanoate) (PHA) polymers (Chart 1) has received increasing academic and industrial interest since the first member of this family, poly(β-hydroxybutyrate) (PHB) (n = 0) was found to be a biodegradable thermoplastic with physical properties similar to those of polypropylene.[1]

Early reports of PHA's with "n" greater than zero were made by Wallen *et al.*,[2] who identified PHA's with 2–4 carbon side chains in activated (aerobic) sewage sludge. Recently, controlled fermentation of *Pseudomonas oleovorans* fed by carbon sources consisting of alkane, 1-alkene,[3] and alkanoic[4] or alkenoic acid salts[5] has yielded PHA's with both aliphatic and olefinic groups in the side chain. The aliphatic side-chain polyesters with chain lengths of 5–7 carbons have been shown to be thermoplastic elastomers[6] from the shape of stress–strain curves and values of the initial modulus for representative samples. Thus, unlike PHB, which is a crystalline thermoplastic[7] and somewhat brittle, these long side-chain polyesters have potential for commercial applications requiring biodegradable plastics with tough elastomeric properties.

All bacterially produced PHA's with n = 3 or more have shown to be composed of at least terpolymers consisting of up to 86% of the monomer used in the feed, with at least 7–10% of a secondary monomer and a few percentage of a third monomer, both of which differ from the feed monomer by ±2 carbon units.[4] The sequence distribution of repeating units of a polyester from nonanoic acid was found to follow Bernoullian statistics which indicates long side-chain PHA's to be random polyesters.[8] From these efforts, it is clear that all properties of and measurements made of these bacterial PHA's are representative of a random terpolymeric system rather than of a pure homopolymer based on the feed monomer.

Past studies have shown that synthetic PHB produced by the ring opening of (±)-β-butyrolactone[9] has properties very similar to that of bacterial PHB (available as 100% homopolymer). The primary differences is that the synthetic polymer is optically inactive and consists of a random stereoblock of *R* and *S* units, whereas the bacterial polyester is optically active and 100% *R* in configuration. The focus of the study in this paper is to prepare synthetic polyesters with long side-chain aliphatic pendant groups from lactones and compare these "homopolyesters" with those synthesized in nature. In an unpublished work, Perez and Lenz have synthesized a nonbacterial poly(β-hydroxyoctanoate) (PHO), with all *R*, all *S*, and a mixture of *R* and *S* optical configuration.[10] In our work, a synthetic poly[(*R*,*S*)-β-hydroxyheptanoate] (PHH) and poly[(*R*,*S*)-β-hydroxynonanoate] (PHN) are prepared from the ring opening of (±)-β-heptanolactone and (±)-β-nonanolactone, respectively.

Chart 1

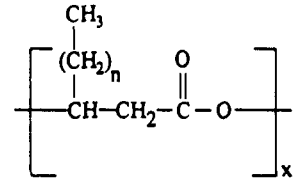

Experimental Section

Materials. All chemicals, except the lactones, were obtained commercially from the Aldrich Chemical Co. Aldehydes were purified by vacuum distillation, with the first few milliliters of distillate being disposed of so as to ensure removal of residual water. Dry pyridine and purified aldehydes were stored over 4-Å molecular sieves until required. Reagent-grade malonic acid was crushed prior to use and needed no further purification. Dry hydrogen bromide was purchased with greater than 98% purity or prepared prior to use from sodium bromide and sulfuric acid. All lactones synthesized were dried over 4-Å molecular sieves prior to use. Trimethylaluminum (2 M) in toluene was used as purchased and mixed with distilled water to form the polymerization catalyst.

Lactone Synthesis. A standard three-step synthesis was followed as shown in Scheme 1.[9]

The first step was a 3–7-day Knoevenagel reaction which was conducted under nitrogen at room temperature and was complete upon cessation of carbon dioxide liberation. The olefinic acid was obtained in 40–70% yield after purification by fractional distillation at reduced pressure. Next hydrogen bromide was bubbled through the olefinic acid for a total of 6 h over a period of 4–6-days to form the β-bromo acid in excess of 80% yield. The

* To whom all correspondence should be addressed.
® Abstract published in *Advance ACS Abstracts*, March 15, 1994.

0024-9297/94/2227-2595$04.50/0

Scheme 1. General Three-Step Reaction Sequence for the Preparation of β-Lactones

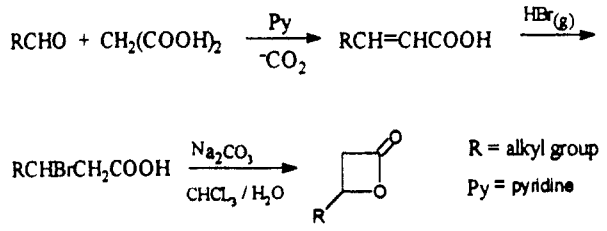

progress of this reaction was monitored by proton NMR. Finally, the bromo acid is cyclized by intramolecular substitution under phase-transfer conditions at 40 °C for 1–4 days to yield the β-lactone in 25–50% yield after Kugelrohr distillation. Due to the difficulty in purifying the high-boiling β-bromoheptanoic and -nonanoic acids, even under high vacuum, the crude acids were lactonized after sufficient degassing under vacuum to remove any excess solubilized hydrogen bromide gas from the previous step. The formation of the lactone can be monitored by proton NMR and infrared spectroscopy during the course of the reaction.

Lactone Polymerization. Polymerization of the lactones was via ring-opening polymerization used an *in situ* aluminum methyl/water catalyst. The reaction was conducted in stoppered ampules following the general format described in an earlier paper.[11] Reactions were conducted with lactones on a 50–70 mmol scale with 5 mol % of catalyst relative to lactone. The specifics of note for the present reactions are as follows:

1. The order of addition of reagents was aluminum alkyl followed by water and then lactone for (±)-β-heptanolactone polymerization, whereas the lactone and water were mixed prior to the addition of aluminum alkyl in the (±)-β-nonanolactone polymerization. Five mole percent of the 1:1 aluminum trimethyl/water *in situ* catalyst, with respect to the lactones, was used in both polymerizations.

2. A final pressure of 1×10^{-3} Torr was reached prior to sealing the ampule for the (±)-β-heptanolactone polymerization as compared to only 3×10^{-2} Torr for (±)-β-nonanolactone.

3. The temperature and duration over which the polymerizations were conducted were 40 °C and 6 days, respectively.

4. Workup involved dissolving the product in chloroform containing 5% added acetylacetone followed by precipitation in cold methanol. This was repeated a second time to ensure removal of catalyst residues.

Yields of polymer were 4–6% for PHH and 2% for PHN.

Polymer Characterization. Proton and carbon-13 NMR spectra of 4–5% (w/v) polymer solutions in $CDCl_3$ were recorded on Varian XL-200 and XL-300 spectrometers, respectively, using the same techniques as reported previously.[9] Solid-state carbon-13 NMR spectra were taken on a Chemagnetics CMX-300 spectrometer at 75.3 MHz using a 7.5-mm rotor as in our previous paper.[19] Spectra of crystalline regimes were recorded under conditions of cross polarization/magic angle spinning (CP/MAS), whereas those of the amorphous regimes were recorded using magic angle spinning only. Spinning speeds were approximately 4–5 kHz, with a contact time for cross polarization of 1 ms and a proton decoupler field strength of about 55 kHz.

Thermograms were recorded using a Perkin-Elmer DSC-7 on 3–8-mg samples. Thermograms shown in Figures 3 and 4 were observed after melting by heating to 100 °C and allowing to crystallize for 2 weeks at 0 °C. A heating rate of 20 °C/min over a temperature range of −60 to +105 °C was used over two heat/cool cycles.

Gel permeation chromatography was conducted on a Waters Associates Model 6000 A solvent delivery system, with a Hewlett Packard HP1047A refractive index detector. Five 300 × 7.8 mm Waters Associates μ-Styragel columns (10^6, 10^5, 10^4, 10^3, and 500 Å) connected in series were used in the analysis. The flow rate was set at 1.4 mL/min, and sample concentrations were between 0.2 and 0.3% (w/v) chloroform. All solutions were filtered through 0.45-μm-pore filter units before injection. Injection volumes of 120 μL were used for each analysis. Monodisperse polystyrene standards purchased from Waters/Millipore were used to create a calibration curve.

Wide-angle X-ray powder patterns and fiber diagrams were recorded on samples mounted on a 0.015-in. collimator in an evacuated flat-film Warhus camera. A Philips PW 1730 generator was used to produce Ni-filtered Cu Kα radiation (λ = 1.541 Å). Solvent-precipitated samples required at least 2 weeks at room temperature before showing clear reflections. Clear reflections were also obtained for melt-cast (80–90 °C) samples left at room temperature for 1 week. It was possible to slowly stretch the PHH sample in a mechanical extensometer over a period of 3–4 days at room temperature to 3 times its initial length. A fiber diagram was obtained for the PHH sample held in the mechanical extensometer during X-ray exposure. The sodium fluoride d_{002} reflection was used to calibrate measured sample reflections. Exposure times ranged from 4 to 8 h.

Optical microphotographs were taken using a Nikon Microphot-FXA polarizing microscope with a Nikon FX-35DX camera.

Density was determined by a flotation technique. A stock sodium bromide solution was prepared and its concentration was determined by titrating with water until a standard density bead (1.0500 g/mL, purchased from Ace Glass Co., Vineland, NJ) started to sink into the body of the solution where it remained stationary. The concentration of the stock solution was determined from a least-squares fit of density (1.0099–1.1352 g/mL) versus concentration (0.147–1.765 mol/L) for sodium bromide solutions as tabulated in the *CRC Handbook of Chemistry and Physics*, 58th ed.,[13] and the dilution volume of water used of the titrated solution. Amorphous samples were obtained by heating to 105 °C followed by quenching in liquid nitrogen prior to titration.

Percent crystallinity,[14] α, is defined in eq 1, where ν is the observed specific volume, ν_c is the crystalline specific volume derived from unit cell calculations, and ν_a is the specific volume for the amorphous sample.

$$\alpha = \frac{100(\nu_a - \nu)}{(\nu_a - \nu_c)} \tag{1}$$

Unit cell parameters and Miller indices were obtained by fitting experimental wide-angle X-ray fiber diagram d-spacings from the various layer lines using computer software provided by F. Brisse, Department of Chemistry, Université de Montréal.

Results and Discussion

Appearance/Texture of Polymer Samples. The "as-precipitated" synthetic poly(β-hydroxyheptanoate) and poly(β-hydroxynonanoate) (henceforth, PHH and PHN, respectively) are sticky and rubbery. After vacuum drying at 45–50 °C and allowing a crystallization period of at least 2 weeks at ambient room temperature, both samples are nonsticky, with the PHH more elastic and the PHN more leathery in nature upon manual stretching.

Polarization microscopy revealed the development of anisotropy and poorly defined spherulitic texture in samples melted between 75 and 85 °C and allowed at least 2 weeks to crystallize at 0 °C. Figures 1 and 2 show typical birefringences for PHH and PHN films treated in this manner. The PHH film produces large areas of birefringence (0.1 mm in diameter), but only irregular maltese crosses are visible.

Few isolated spherulites of 0.05 mm or less develop in the PHN sample. The overall appearance between crossed polars was "speckled" and "cross-ply". Bacterial long side-chain polyesters in this family (5–7 carbon side chain) were reported not to show spherulitic textures for samples annealed at 40 °C.[6] Overall, polarization microscopy does not provide evidence for anything but anisotropy. Radial symmetry in the anisotropic domains is poor. The optical texture is reminiscent of nematic and smectic liquid crystals[12] rather than of the highly spherulitic organization found in PHB.

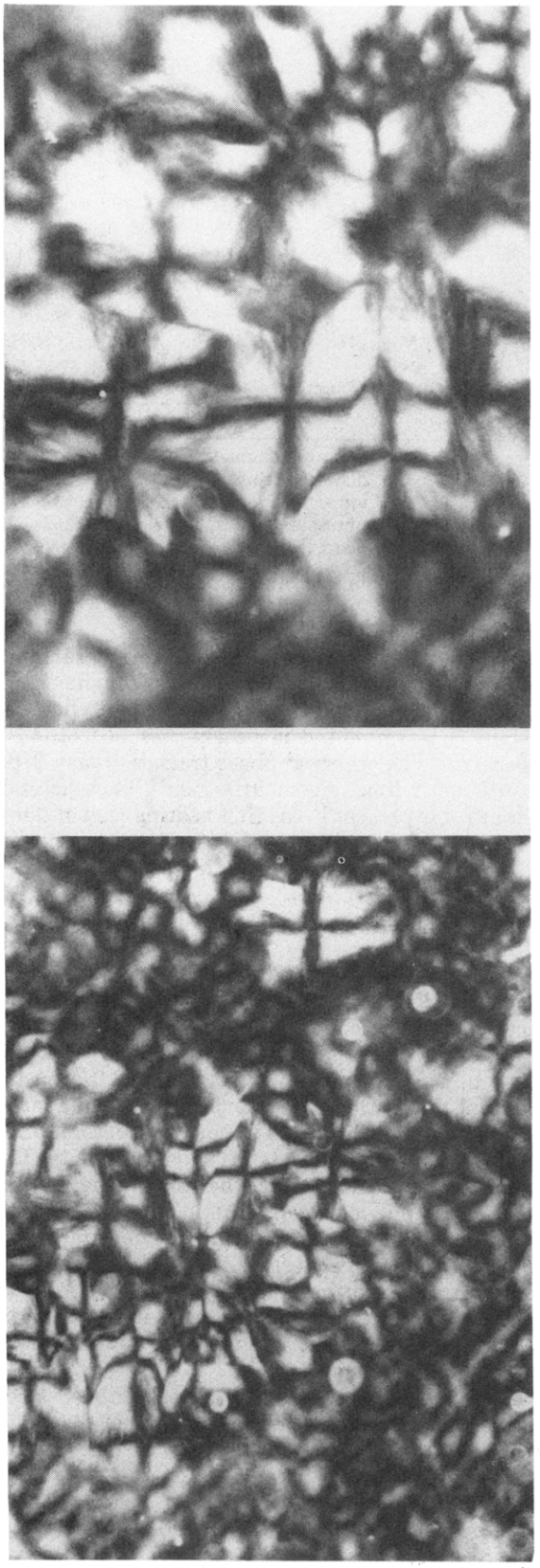

Figure 1. Polarization optical micrograph of a PHH thin film crystallized from the melt over 2 weeks at 0 °C (upper ×400; lower ×200).

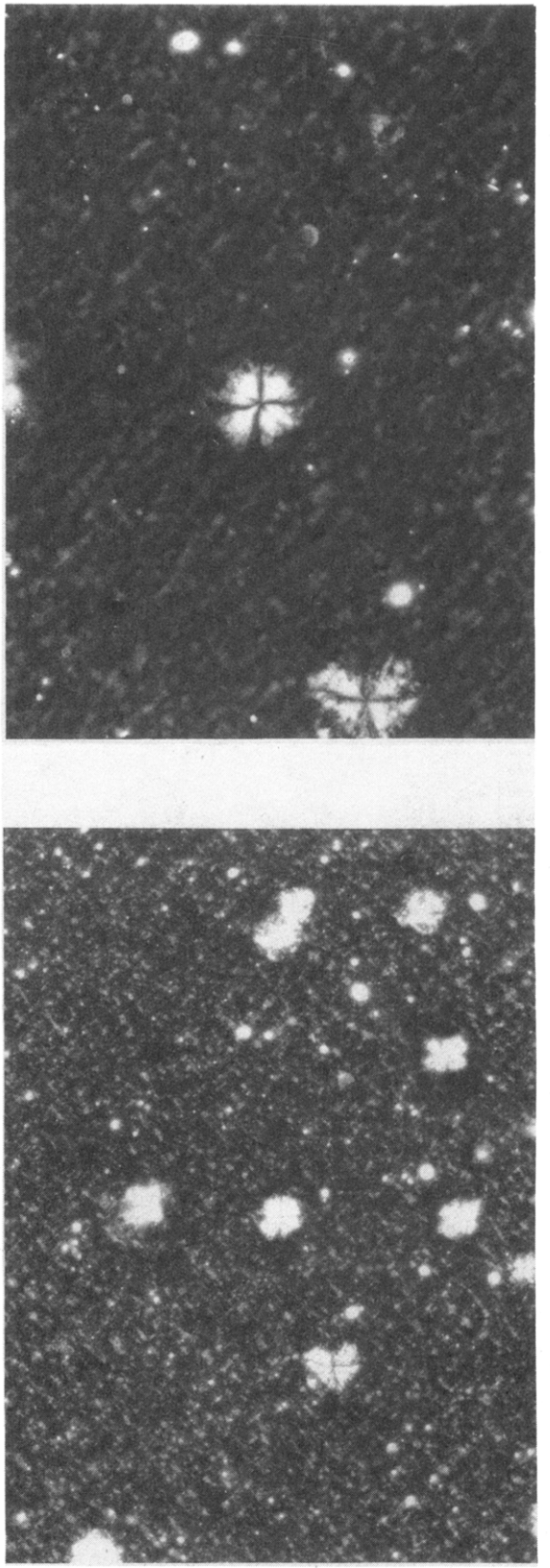

Figure 2. Polarization optical micrograph of a PHN thin film crystallized from the melt over 2 weeks at 0 °C (upper ×400; lower ×200).

Thermal Analysis. Glass transitions and peak melting points for synthetic PHH and PHN samples are listed in Table 1 along with previously reported values for bacterial samples.[4]

The glass transitions for the synthetic polymers and their bacterial analogues are almost identical. The melting points and the enthalpies of fusion are dependent on the degree of crystallinity of the sample, which in turn is subject to the temperature and duration over which crystallization is allowed to take place. Unlike PHB, which crystallizes almost immediately after cooling from the melt,[15] the long side-chain analogues require a much longer period.

Table 1. Thermal Analysis of Synthetic and Bacterial Long Side-Chain Polyalkanoates

sample	T_m peak ± 3% (°C)	T_g onset ± 2% (°C)	ΔH ± 5% (J/g)
synthetic PHH	56	−32	14
synthetic PHN	60	−43	25
bacterial PHH[4]	45	−33	5.4
bacterial PHN[4]	54	−39	22.5

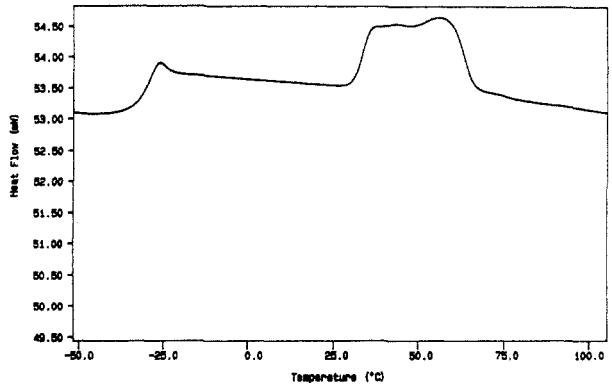

Figure 3. DSC thermogram of the first heating scan of a synthetic PHH sample after melting and recrystallization (2 weeks at 0–5 °C).

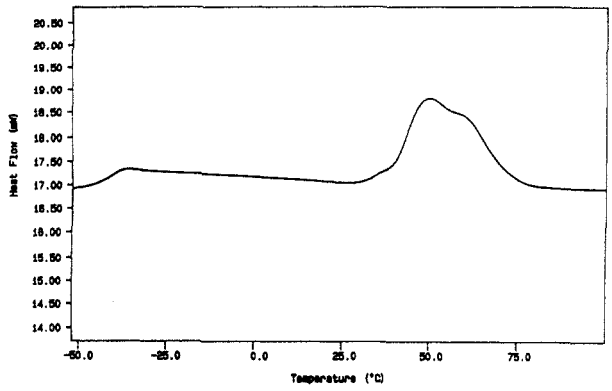

Figure 4. DSC thermogram of the first heating scan of a synthetic PHN sample after melting and recrystallization (2 weeks at 0–5 °C).

Recently, Gagnon *et al.*[16] determined that, for a bacterial copolyester consisting chiefly of poly(β-hydroxyoctanoate), the rate of crystallization, after prior melting at 75 °C, is maximal between 0 and 5 °C. The degree of crystallinity was found to increase with time and level off to reach stable values after 3 weeks. It may be expected, however, that for the synthetic polyesters a shorter crystallization period is necessary as they are 100% homopolymers, unlike the bacterial analogues which contain at least 10–15% comonomers.[4] Therefore, the thermograms of the synthetic samples in this study were rerun after a 2-week crystallization period at 0–5 °C after having previously been melted at 100 °C (Figures 3 and 4). The bacterial samples listed in Table 1 were reported to have been precipitated from solution and dried in vacuo at ambient temperature prior to thermal analysis.[4] The higher recorded melting maxima and heats of fusion of the synthetic samples are very likely the result of the fact that these are homopolymers which have been allowed to crystallize near the optimal conditions of temperature and time found for the bacterial sample consisting chiefly of β-hydroxyoctanoate units. It would be expected that the bacterial samples would have comparable if not higher melting maxima and heats of fusion if pretreated in the same manner prior to analysis.

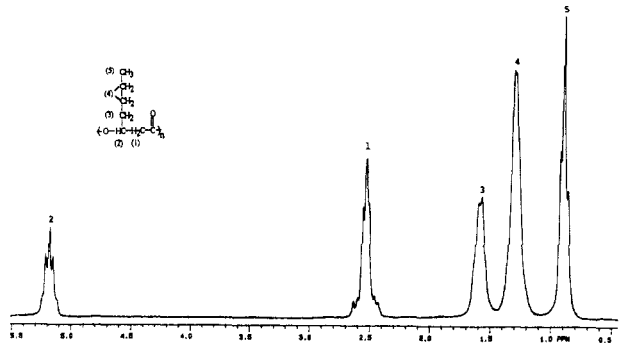

Figure 5. 200-MHz ^{1}H NMR spectrum of synthetic PHH.

Table 2. Proton Chemical Shifts for Synthetic PHH

proton label[a]	nature of signal	shift (ppm)
1	distorted doublet	2.54, 2.51, 2.49
2	distorted triplet	5.20, 5.17, 5.14
3	unresolved multiplet	1.58, 1.55
4	unresolved multiplet	1.28, 1.26
5	distorted triplet	0.90, 0.87, 0.84

[a] Refer to Figure 5 for the nature of proton corresponding to the assigned label.

An interesting feature noted in the thermograms of the synthetic samples was a small secondary higher melting peak between 87 and 88 °C. This peak is barely detectable for the PHH sample but is clearly present in the PHN endotherm. The observed phase transition may depend on a sufficiently long side-chain length.[17] These secondary peaks are only present in the first heating scan of samples that were precipitated from chloroform and subsequently solvent exchanged with water and freeze dried (refer to the Experimental section). They do not appear after the samples are allowed to recrystallize from the melt at 0–5 °C for 2 weeks.

Solution NMR. The solution proton NMR spectrum of synthetic PHH is shown in Figure 5 along with peak assignments. The chemical shifts listed in Table 2 are comparable to bacterial samples[3,4] which are copolyesters of several long-chain monomers. Unlike the bacterial polyesters, the synthetic polymer can be prepared as 100% PHH homopolymer, which accounts for some of the differences in peak chemical shift and multiplicity. Other differences are due to the fact that the synthetic PHH is a stereoblock polymer, consisting of blocks of *R* and *S* polymer chains arising from the polymerization of a racemic lactone with a stereoregulating catalyst system.[9] The spectrum of synthetic PHN is virtually identical to those of synthetic PHH with the exception of relative peak integration which reflects the two additional methylene units in the side chain.

The carbon-13 solution spectrum of synthetic PHH is shown in Figure 6 along with peak assignments. Chemical shifts listed in Table 3 are essentially identical to those of bacterial analogues reported by Gross *et al.*[4] The principal difference is that there are two carbonyl signals for the synthetic samples due to diad tacticity effects.[9] The percent isotactic diads are as calculated in eq 2, where A_h is the area under the high-field ^{13}C carbonyl NMR signal and A_l the area under the low-field signal.

$$\% I = \frac{A_h \times 100}{(A_h + A_l)} \qquad (2)$$

This is 82 ± 5% for PHH and 80 ± 5% for PHN. The significance of these figures is that the whole unfractionated polymer is highly isotactic *RR,SS* with a small

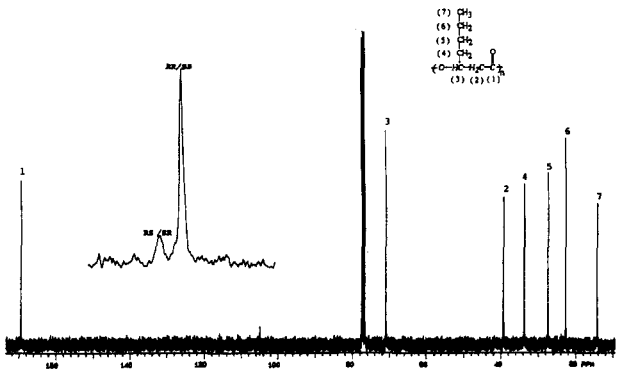

Figure 6. 75.3-MHz ^{13}C NMR spectrum of synthetic PHH with expansion of the carbonyl signal shown.

Table 3. Solution Carbon-13 Chemical Shifts for Synthetic PHH and PHN[a]

carbon label[b]	shift for PHH (ppm)	shift for PHN (ppm)
1	169.52, 169.40	169.49, 169.37
2	39.11	39.09
3	70.82	70.82
4	33.49	33.79
5	27.15	25.00
6	22.42	29.04
7	13.92	31.68
8		22.56
9		14.03

[a] Relative to internal TMS. [b] Refer to Figure 6 for the nature of carbon corresponding to the assigned number.

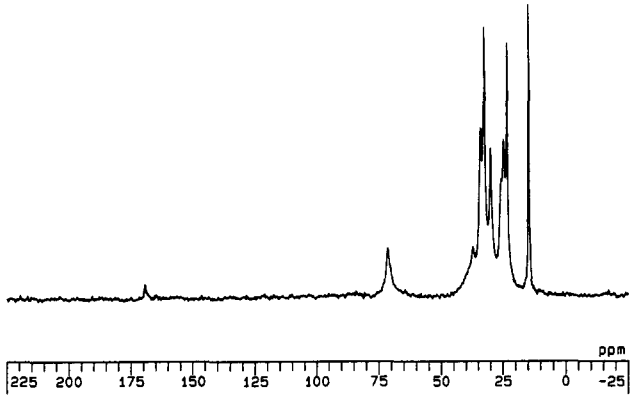

Figure 7. 75.3-MHz solid-state ^{13}C NMR spectrum of synthetic PHN under conditions favoring resonances due to a noncrystalline domain (MAS) (probe background signals were removed by a spin–echo pulse sequence).

proportion of the downfield *RS,SR* syndiotactic diad content. Fractionation of these polymers was not attempted due to the limited availability of the sample. This would be expected to yield a fraction with a higher percentage isotactic diad content, more closely resembling bacterial counterparts as found for synthetic poly(β-hydroxybutyrate).[9]

Solid-State NMR. Solid-state carbon-13 NMR spectra were acquired to distinguish between crystalline and noncrystalline regimes in the synthetic PHH and PHN samples. Figure 7 shows the spectrum of PHN taken using single-pulse Bloch decay and magic angle spinning (MAS), favoring signals due to the noncrystalline polymer component. Figure 8 shows the sample spectrum recorded under cross polarization/magic angle spinning conditions which also allows signals from the crystalline regions to become visible. Both crystalline and noncrystalline shifts are tabulated in Table 4. The chemical shifts of the noncrystalline regions correlate well with the solution NMR as would be expected for solid samples well above their glass transition temperatures.[18] These results concur

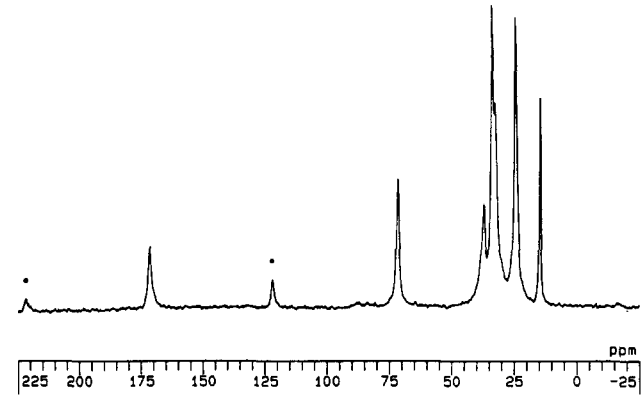

Figure 8. 75.3-MHz solid-state ^{13}C NMR spectrum of synthetic PHN under conditions favoring resonances due to a crystalline domain (CP/MAS) (the asterisks show spinning side bands).

Table 4. Carbon-13 Solid-State Chemical Shifts for Synthetic PHH and PHN

	shifts for PHH (ppm)		shifts for PHN (ppm)	
carbon label[f]	solid-state crystalline	solid-state amorhous	solid-state crystalline	solid-state amorhous
1	179.09	169.03	171.39	168.84
2	41.6 (37.21[a])	38.82	36.51[b]	36.75
3	71.28[b]	70.94	71.06[b]	70.99
4	32.70 (33.71[a])	33.58	33.40[b]	33.40
5	25.69 (27.44[a])	27.15	24.06[c]	25.06
6	24.56 (23.43[a])	22.48	32.12[b]	29.31
7	15.42 (13.92[a])	13.92	32.12[b,c]	31.94
8			24.06[c]	22.69
9			14.13[b]	14.03
	30.07[d]			24.06[e]

[a] Signal due to an amorphous component which has not been suppressed in the CP/MAS experiment. [b] Tentatively assigned to carbon in the crystalline domain. [c] Signal due to more than one carbon. [d] Unassigned peak. [e] Signal due to a crystalline component which has not been suppressed in the MAS experiment. [f] Refer to Figure 6 for carbon numbering.

with those of Morin and Marchessault,[19] who have done similar experiments with a bacterial polyester consisting chiefly of octanoate units.

The CP/MAS spectrum of PHN (Figure 8) shows peaks due to crystalline domains not seen in the MAS only experiment. These peaks typically differ by a few ppm from the corresponding carbons in the amorphous regimes. Even in the CP/MAS spectra, the methyl carbons of the amorphous domains are still present and are more intense than those of the crystalline domains. This indicates an appreciable amorphous content in this sample.

Due to the similarities in solid-state spectra of the synthetic samples with the bacterial analogues, more detailed experiments into T_1 and T_2 values for these polymers are warranted in order to obtain quantitative information on correlation times for motions of the backbone and side-chain carbons and to provide insight into the molecular dynamics as affected by tacticity.

X-ray Diffraction Studies of Synthetic PHH and PHN Polymers. The fiber diagram of PHH shown in Figure 9 (schematic) corresponds to the data in Table 5, calculated using Bragg's law from the experimental diffractogram. The orthorhombic unit cell was derived assuming conformation and packing similar to those for long side-chain bacterial polyesters.[6] Thus the meridional reflection on the second layer line was taken as support for the 2_1 helical conformation since there was no evidence for a well-defined first layer line meridional. Fiber-tilting experiments were performed to support these observations. The pitch of the 2_1 helix was 4.55 Å, which is very similar to that of the bacterial PHO.[6]

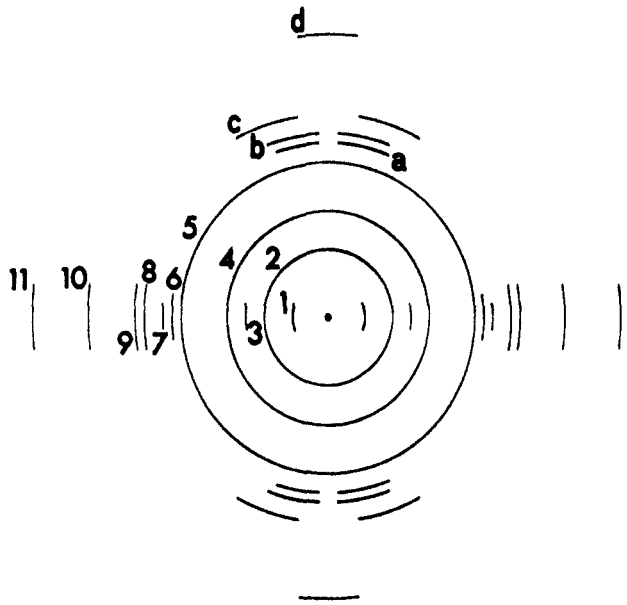

Figure 9. Schematic wide-angle diffraction pattern of oriented syntehtic PHH (*d* spacings and observed reflection intensities listed in Table 5).

Table 5. Experimental *d* Spacings of Synthetic PHH Polymer (cf. Schematic Fiber Diagram: Figure 9)

	PHH *d*, Å			
ref. no.	measd	calcd	intensity of reflections	Miller indices
1	16.19	15.63	very strong	020
3	7.71	7.81	very weak	040
6	4.94	5.19	strong	110
7	4.74	4.70	medium	130
8	4.34	4.36	strong	140
9	3.89	3.90	moderate	080
10	3.10	3.13	weak	180
11	2.60	2.63	weak	200
a	4.59	4.50	weak	011
b	4.34	4.37	medium	021
c	4.10	4.17	strong	031
d	2.23	2.27	very weak	002
2[a]	9.22		weak	
4[a]	6.54		weak	
5[a]	5.21		very weak	

[a] These reflections observed in Figure 9 do not orient upon stretching of the sample and were not used in unit cell calculations. The possible origin of these lines is proposed in the Discussion section.

Table 6. Unit Cell Parameters for Synthetic PHH and Some Bacterial Polyesters

sample[a]	*a* (Å)	*b* (Å)	*c* (Å)	*R*-factor (agreement factor)
PHH synthetic	5.26	31.25	4.55	0.348
PHO bacterial[6]	5.12	36.05	4.55	0.255
PHN bacterial[6]	5.24	38.46	4.57	0.275
PHD bacterial[6]	5.15	40.01	4.55	0.296

[a] PHH: poly[(*R*,*S*)-β-hydroxyheptanoate].

In Table 6, unit cell parameters of various bacterial PHA's are shown for comparison with synthetic PHH. The agreement factor, which provides a measure of the deviation between experimental and measured reflections used in calculating the unit cell dimensions, is slightly worse for the synthetic PHH, compared to those reported for the bacterial polyesters.[6] This is likely due to imperfections in the unit cells of the synthetic polymer, due to the packing of stereoblock macromolecules possessing blocks of *R* and *S* repeating units of varying lengths which are assumed to segregate into crystals of either *R* or *S* chirality. The imperfect segregation in such a system probably also accounts for greater dispersion in *d* spacings

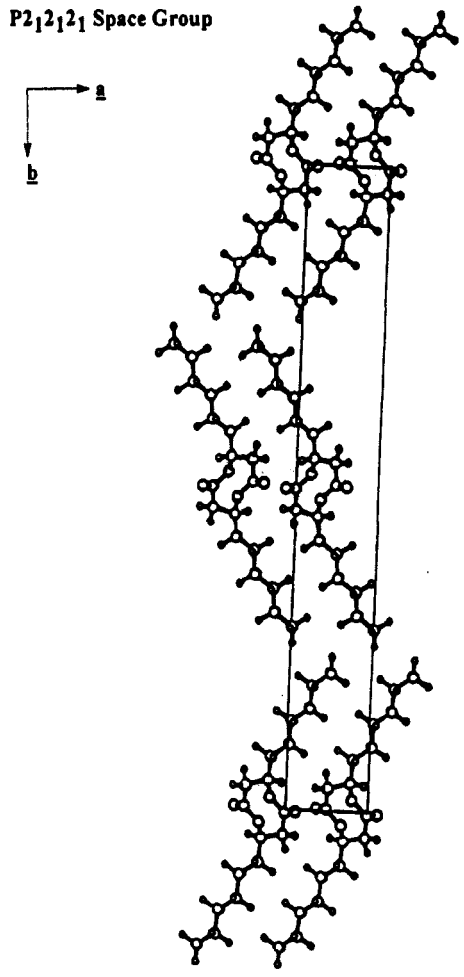

Figure 10. Base plane projection of the unit cell of PHN with a comblike conformation.

than in the corresponding bacterial samples which are 100% *R* in configuration.

The packing of the side chain in these polyesters can be related to crystallization of isotactic long side-chain unbranched polyolefins.[20] Polytetra-, polyhexa-, and polyoctadecene-1 were found to crystallize in two forms whereby the main chains are aligned in planes and the side chains are extended on either side of the main-chain axis in a parallel array. In the orthorhomobic form, the main chain is helical and the side chains are 130.6° to the helical axis ("herringbone" conformation). In the second form, the side chains are at right angles to the main chain ("comb" conformation). Polydodecene-1, polydecene-1, and polynonene-1 crystallize in this form. Recent conformational analysis on long side-chain PHA's has shown that, in terms of energetics, there is only 1 kcal/mol separating the comb from the herringbone conformation.[6] The comb conformation is shown in an energy-minimized packing projection in Figure 10.

From Table 6, it is noteworthy that the c axis of the unit cells is the same in all cases, indicating that the pitch of the 2_1 helix of this homologous system, starting with PHB (c = 5.96 Å), has been compressed by intramolecular van der Waals attraction between neighboring side chains to a limiting value of 4.55 Å.[6] The *b* dimension of the unit cell increases with the average side-chain length as expected for an extended conformation. Figure 11 depicts the relationship between measured 020 reflections (approximately *b*/2 in Figure 10) and the average number of side-chain carbons for known bacterial samples with the synthetic PHH and PHN polyesters. The line drawn excludes the point for *N* = 2 (PHV) which packs differently

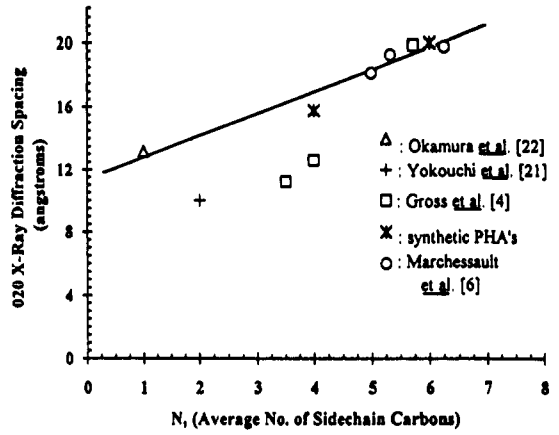

Note : (asterisks are for synthetic polymers prepared in this report; other symbols are for natural bacterial polymers); equation of regression line: y = 1.39 x + 11.4

Figure 11. Regression plot of 020 X-ray diffraction spacing versus average number of side-chain carbons for the polyalkanoate family of polymers.

than the other biopolyesters;[21] the points for $N = 3.5$ and $N = 4$ for the bacterial copolyesters are also neglected due to the fact that these were measured from reflections which were very broad[4] and are subject to more uncertainty than the others. The y-intercept (11.4 Å) should correspond to the intermolecular packing of poly(β-hydroxypropionate), where $N = 0$, but verification was not possible as this spacing has not been reported in the literature. A similar plot has been published for isotactic polyolefins with unbranched side chains and was found to be linear.[20]

Of note in the schematic fiber diagram of synthetic PHH (Figure 9) are unoriented reflections. The origin of these reflections is not clear; hence, they were not used in deriving the unit cell. They may relate to a small endotherm observed between 85 and 90 °C (mentioned in the Thermal Analysis section above) which is possibly a second crystalline phase. The same reflections are clearly present in the powder diffraction patterns (not shown). The flat-film powder X-ray patterns of synthetic PHH and PHN have extra reflections compared to bacterial PHO. This may reflect differences in space groups or other phases, and interpretation must await a more detailed analysis. Caution should be used in identifying molecular species *via* powder diffractograms. In PHA samples the most intense reflection has the longest d-spacing and corresponds approximately to the width of the ribbonlike 2_1 chain, with the extended aliphatic side chains. It is the only reflection which changes systematically with the composition (Figure 11).

Density Measurements. The measured density of synthetic PHH was found to be in accord with the general trend of decreasing density with side-chain length as indicated in Table 7. As the side-chain length increases, the density approaches that of polyolefins, which is indicative of packing in polyethylene-like domains.

From the unit cell dimensions, the theoretical density of synthetic PHH was calculated.[22] This result is a value of 1.138 g/cm³. The experimentally measured density of synthetic PHH of 1.105 ± 0.002 g/cm² is reasonable as the polymer will always have some amorphous content which reduces the measured density from the theoretical value based on a 100% crystalline polymer.

The percentage degree of crystallinity, α, of the synthetic PHH can thus be calculated to be 41% from eq I using $(1.083\ g/cm^3)^-$ for ν_a (determined as described in the Experimental Section) and $(1.138\ g/cm^3)^{-1}$ for ν_c. The sample was allowed to stand for 4 weeks at 0–5 °C, which parallels what Gagnon *et al.*[16] found to be optimal for maximal crystallization of a bacterial PHO sample—3 weeks at 5 °C.

Table 7. Density Measurements of Some Bacterial and Synthetic Polyalkanoate Polyesters

sample	average side-chain length[a]	density (±0.002 g/cm³)
PHB synthetic	1.00	1.232
PHB bacterial[6]	1.00	1.243
PHV bacterial[6]	2.00	1.200
PHH synthetic	4.00	1.105
PHH synthetic (amorphous)	4.00	1.083
PHO bacterial[6]	4.99	1.019
PHN synthetic	6.00	1.018
PHN bacterial[6]	5.32	1.026
PHD bacterial[6]	6.25	1.033

[a] Relates to the fact that some long side-chain bacterial samples are not 100% homopolymer and contain small quantities of other polyesters of varying side-chain length.[4]

Table 8. Molecular Weights of Synthetic and Bacterial Polyesters Samples

sample	mol wt at midpoint of chromatogram profile (±10%)	width of chromatogram profile (min)
PHH synthetic	550 000	3.6
PHN synthetic	740 000	5.5
PHO bacterial[a]	190 000	3.9

[a] This sample was provided by Dr. B. A. Ramsay.

Gel Permeation Chromatography. Table 8 shows the calculated molecular weights at the midpoint of the GPC chromatogram profile for synthetic PHH, PHN, and bacterial PHO samples.[23] The synthetic samples have 3–4 times the molecular weight of the bacterial PHO at this point in the chromatogram. A complete calculation of weight- and number-average molecular weights was not attempted, as ideally a universal calibration curve is required for more accurate molecular weight determinations.[24] This relies on knowledge of the polymers' Mark–Houwink constants, which have not been determined for these new polyesters.

An estimate of the polydispersity of the samples was determined as the time required for the chromatogram to return to the base line after sample detection. The synthetic PHH is comparable to the bacterial PHO in this respect, but the dispersity of the synthetic PHN is roughly twice that of the other two. This sample also had a nonsymmetric GPC profile skewed to the high molecular weight end, whereas the synthetic PHH and bacterial samples had fairly symmetric profiles. Other workers have isolated bacterial PHO and report weight-average molecular weights of between 160 000 and 180 000.[3,4]

Conclusions

Synthetic long side-chain PHA's possessing four and six carbon aliphatic pendant side chains have been shown to have physical properties very similar to those of the bacterially produced analogues. Although optically inactive, these materials, unlike the bacterial polyesters, are homopolymers which allow one to correlate physical properties of the sample with one monomeric constituent. The unit cell dimensions for the synthetic PHH were worked out based on those of bacterial samples, and it was shown that packing is similar in these samples. The WAXD powder pattern, however, shows extra reflections not seen in the corresponding patterns of the natural polymer at angles less than 24° 2θ. The fiber diagram also shows three unoriented reflections at 2θ less than 18° which were not included in the unit cell determination. In

addition, the DSC thermograms show small secondary melting above the main polymer melting endotherms. This suggests that the side chains may form liquid-crystalline-like domains upon crystallization.

Acknowledgment. We thank Dr. Juanita Parris and Mr. Michel Pelletier for discussions and assistance in determining the unit cell parameters from the X-ray patterns of the synthetic PHH polymer. Also we acknowledge the aid of Dr. Fred Morin of the Chemistry Department, McGill University, in acquiring the solid-state NMR spectra. Financial assistance was provided by NSERC and the Xerox Corp.

References and Notes

(1) Le Borgne, A.; Spassky, N. In *Models of Biopolymers by Ring Opening Polymerization*; Penczek, S., Ed.; Chemical Rubber Corporation: West Palm Beach, FL, 1990; p 238.
(2) Wallen, L. L.; Rohwedder, W. K. *Environ. Sci. Technol.* **1974**, *8*, 576.
(3) Preusting, H.; Nijenhuis, A.; Witholt, B. *Macromolecules* **1990**, *23*, 4220.
(4) Gross, R. A.; Demello, C.; Lenz, R.; Brandl, H.; Fuller, C. *Macromolecules* **1989**, *22*, 1106.
(5) Fritzsche, K.; Lenz, R. W.; Fuller, R. C. *Int. J. Biol. Macromol.* **1990**, *12*, 85.
(6) Marchessault, R. H.; Monasterios, C. J.; Morin, F. G.; Sundararajan, P. R. *Int. J. Biol. Macromol.* **1990**, *12*, 158.
(7) Barham, P. J.; Keller, A. *J. Polym. Sci., Polym. Phys. Ed.* **1986**, *24*, 69.
(8) Ballistreri, A.; Montaudo, G.; Guiffrida, M.; Lenz, R. W.; Kim, Y. B.; Fuller, R. C. *Macromolecules* **1992**, *25* (7), 1845.
(9) Bloembergen, S.; Holden, D. A.; Bluhm, T. L.; Hamer, G. K.; Marchessault, R. H. *Macromolecules* **1989**, *22*, 1656.
(10) Lenz, R. W. Polymer Science and Engineering Department, University of Massachusetts, Amherst, MA, private communication.
(11) Jesudason, J. J.; Marchessault, R. H.; Saito, T. *J. Environ. Polym. Degrad.* **1993**, *1* (2), 89.
(12) Noel, C. In *Side Chain Liquid Crystal Polymers*; McArdle, C. B., Ed.; Chapman and Hall: New York, 1989; p 159.
(13) *CRC Handbook of Chemistry and Physics*; Weast, R. C., Ed.; Chemical Rubber Corp.: West Palm Beach, FL, 1977; p D-251.
(14) Billmeyer, F. W. *Textbook of Polymer Science*; John Wiley and Sons: New York, 1971; p 173.
(15) Barham, P. J. *J. Mater. Sci.* **1984**, *19*, 3826.
(16) Gagnon, K. D.; Lenz, R. W.; Farris, R. J.; Fuller, R. C. *Macromolecules* **1992**, *25*, 3723.
(17) Plate, N. A.; Shibaev, V. P. In *Comb-Shaped Polymers and Liquid Crystals*; Plenum: New York, 1987.
(18) Duch, M. W.; Grant, D. M. *Macromolecules* **1970**, *3*, 165. Schaefer, J. *Macromolecules* **1972**, *5*, 427.
(19) Morin, F.; Marchessault, R. H. *Macromolecules* **1992**, *25*, 576.
(20) Turner Jones, A. *Makromol. Chem.* **1964**, *71*, 1.
(21) Yokouchi, M.; Chatani, Y.; Tadokoro, H.; Tani, H. *Polym. J.* **1974**, *6* (3), 248.
(22) Okamura, K.; Marchessault, R. H. In *Conformation of Biopolymers*; Ramachandran, G. N., Ed.; Academic: London, 1967; Vol. 2, p 709.
(23) Ramsay, B. A.; Saracovan, I; Ramsay, J.; Marchessault, R. H. *Appl. Environ. Microbiol.* **1991**, *5* (3), 625.
(24) *Modern Size-Exclusion Liquid Chromatography: Practice of Gel Permeation and Gel Filtration Chromatography*; Yau, W. W., Ed.; Wiley: New York, 1979; p 291.